Farhana Anjum, Saima Gul, Mohammad Iqbal Khan and Murad Ali Khan*

Efficient synthesis of palladium nanoparticles using guar gum as stabilizer and their applications as catalyst in reduction reactions and degradation of azo dyes

Abstract: Palladium is very expensive metal and has numerous applications especially as a versatile hydrogenation and dehydrogenation catalyst for chemical reactions. The main hurdle in its wide use is the high materials cost. In the present study a cost effective palladium nano catalyst was prepared using the green method of synthesis with guar gum as capping and reducing agent. The formations of palladium nanoparticles were confirmed by UV-spectrophotometer while for morphology and nature, SEM and XRD were performed that confirmed the crystalline nature of PdNPs and proved the roughly spherical shape of nanoparticles. FT-IR analysis showed different functional groups of reducing agent and proved that guar gum have the ability to stabilized as well as to reduce the Pd (II) to Pd (0). Specific signal for the palladium is present in EDX spectra that further confirmed the formation of PdNPs. The catalytic efficiency was studied using the hydrogenation of 4-nitrophenol. Rate constant of prepared nano-catalyst was 0.1436/min, its efficiency, TON, TOF, in above mention reaction is 90.83, 27.78, and 185.2/hrs, respectively. Data obtained proved synthesized PdNPs to be efficient heterogeneous catalyst for the reduction of 4-NP and for the degradation of azo dyes.

Keywords: palladium nano-particles; reduction; degradation; azo dyes

1 Introduction

Palladium is one of the precious and expensive elements and has found extensive usage in industries and laboratories due to its capability of catalyzing various cross coupling reactions [1]. Palladium has truly revolutionized the ways molecules are put together and constructed. Palladium is an outstanding hydrogenation and dehydrogenation catalyst in organometalic chemistry. Apart from chemical reactions palladium has found its way in other fields like electronics and chemical processes [2]. Its use in industrial process may give a new turn to the progress of new technologies [3]. Palladium as a catalyst is used in various industrial processes Petrolium cracking [4], alkaline oxidation, selective low oxide formation [5,6], reduction of C≡C to C=C without further reduction to carbon-carbon single bond (known as Landler's Catalyst) [7], Suzuki coupling [8], Heck reaction [9] and carbon–fluoride bond formation [10]. For the oxidation of alcohols palladium is considered excellent electro-catalyst in alkaline medium [11-14]. Palladium is amalgamated with a wide variety of ligands and used for selective chemical transformation. Akira Suzuki, Richard F. Heck and Ei-ichi Negishi in 2010 obtained Nobel Prize for their work on palladium.

Palladium is a member of platinum group that is considered as one of expensive noble metals and its high material cost generally restricts its wide applications. The cost of the reaction may either be controlled to replace the palladium with cheaper metals or using palladium nanoparticles. The emergence of nano science has engrossed the interest of researchers throughout the world. nano science changes the properties of materials both qualitatively and quantitatively compared with their bulk counterpart, as these nanosized particles are resultant of manipulation at atomic or molecular level. Consequently nowadays trend is going toward nanoparticles. Thus metallic nanoparticles can be stabilized and synthesized through a number of methods including physical and chemical methods, photochemical reduction, mechanical, and electrochemical techniques [15-21]. The scarcity of resources and the rising pollution has forced researchers to look for inventive, eco-friendly procedures and techniques that protect human health and environment. Among

* Corresponding author: Murad Ali Khan, Department of Chemistry, Kohat University of Science and Technology, KPK, Pakistan, email: drmalikhan@yahoo.com, tel. +92-922-52914449
Farhana Anjum, Saima Gul and Mohammad Iqbal Khan, Department of Chemistry, Kohat University of Science and Technology, KPK, Pakistan

those techniques and procedures the preparation of efficient, cost-effective and green catalyst is a challenging [22]. To expand the stability and efficiency of metallic nanoparticles, an efficient and eco-friendly capping or stabilizing agents should be used. Plant materials have been considered a reliable source and a green route for metal nanoparticles synthesis. It is clear from the previous reports that plants and its parts have been successfully utilized for rapid and extracellular synthesis [23]. Green synthesis of palladium nanoparticles is very attention-grabbing because it is cost effective, reduce the use of chemicals, and environmentally benign. All these factors prompted us to explore guar gum (green source) for the synthesis of palladium nanoparticles. PdNPS were earlier synthesized through green approach by using *Cinnamom zeylanicum* bark [24], broth of *Cinnamom camphora* leaf [25], banana peel extract [26], *Annona squamosa* L. peel extract [27], gum acacia [28], *Anacardium occidentale* [29] *Pulicaria glutinosa* extract [30], carboxy methyl cellulose [31], chitosan [32], and xanthan gum [33]. In our study we use guar gum as capping and stabilizing agent for the palladium nanoparticles synthesis. Guar bean is found mostly in India, Pakistan, U.S., Australia and Africa. It is a high molecular weight polysaccharide that is chemically composed of sugar galactose and mannose. The backbone of this polysaccharide is a linear chain of β 1,4-linked mannose residue while the galactose residues are 1,6-linked at every second mannose, giving short side-branch as shown in Figure 1.

Nitro-phenol is the chemical of demand that is not only utilized in the manufacturing of drugs, explosives, dyes and insecticides but also as corrosion inhibitor of wood and rubber [34]. 4-nitrophenol (4-NP) is also used as an intermediate for the synthesis of several useful organic compounds. Para-aminophenol (4-AP) is one of the effective and powerful pharmaceutical intermediates for valuable analgesics synthesis [35]. As 4-nitrophenol is a common precursor for para-aminophenol. Cheaper and novel technique for the catalytic reduction of 4-nitrophenol

is constantly in demand. Catalytic hydrogenation of 4-nitrophenol by NaBH4 has previously been performed by means of gold (Au) nanoparticles deposited on poly methyl methacrylate (PMMA) [36], Au/polypyrrolenano-tubes [37] Ag/SBA-15 [38,39]. and Pd/polypyrrolenano capsules [40], fabricated graphene–carbon sphere hybrid aerogel decorated with silver nanoparticles (G/AgCS) [41], used layer-by- layer polypeptide assemblies to mediate the synthesis of Au/mesoporous silica nanotubes with the apparent rate constant of 3×10^{-4} and $8 \times 10^{-4}\,s^{-1}$ for Au/SNTs obtained from (Lys340/Glu125)5 and (Lys340/PLT)5 coated membranes. In the present study, we reported the catalytic activity of green synthesized PdNPs in reduction of 4-NP to 4-AP Comprehensively in addition, the same catalyst was also used in the reduction of hazardous azo dyes and proved that the palladium is the metal of future.

2 Experimental

2.1 Reagents and material

Guar gum powder and palladium chloride (PdCl$_2$) were purchased from Sigma-Aldrich and used without further purification. For the synthesis of nanoparticles analytical grade solvents like ethanol and methanol were used. The deionized water was obtained from the department Millipore-Q water purification system (18.2MΩ.cm@25 C, TOC < 10 ppb). The reaction tubes were wrapped in aluminum foil to protect it from light.

2.2 Synthesis of palladium nanoparticles

Guar gum (1 g) was dissolved in EtOH (50 mL) at room temperature in a round bottom flask. Then added 10 mg of PdCl$_2$ dissolved in EtOH and refluxed for 2 h. A color change of the mixture from white to dark grey was observed indicating the reduction of palladium ions.
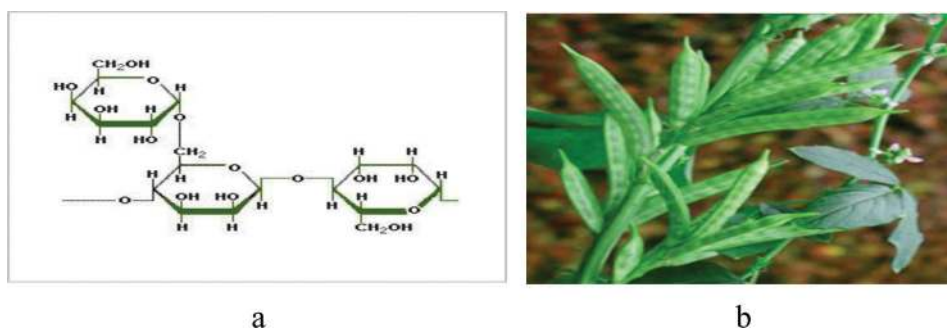

Figure 1: (a) Chemical structure of guar gum. (b) Guar gum plant.
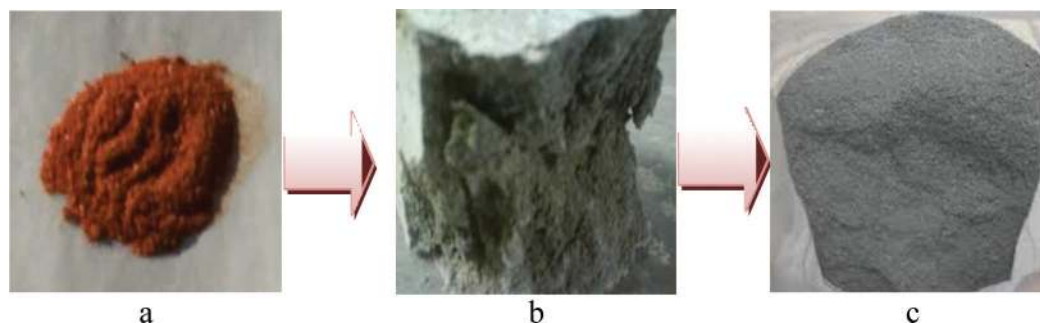
Figure 2: (a) PdCl$_2$, (b) PdNPs in colloidal form, (c) PdNPs in powder form.

This solution was allowed to cool to room temperature. Reduction of palladium chloride was further confirmed by UV spectroscopic analysis in the range of 300-700 nm [42]. The colorimetric change can be observed in Figure 2.

The resultant dark grey color product was centrifuged at 800 rpm for 10 min; supernatant solution was discarded and the resulting PdNPs were washed with deionized water three times followed by washing with methanol and acetone, for removal of any substance adsorbed on the surface of the particles and then centrifuged the mixture to collect the final clean product. The resulted PdNPs were first dried at room temperature and then in the oven at 70°C for 2 h.

2.3 Instrumentation

For weighing the substances electrical balance (AR140 USA) was used, while electric oven Memmert D-91126 Schwabach FRG (Germany) was used for drying of nanoparticles. For the confirmation of formation of PdNPs and its catalytic activity measurement UV-visible spectrophotometer Shimadzu, UV-1800 (Japan) was used. The particles were centrifuged and washed using sigma 1-14 (Germany) centrifuge machine. FT-IR spectral analysis was done by a spectrum-100 FT-IR spectrophotometer from Bruker (ALPHA, USA) using KBr pellets method for nanoparticles within a fixed spectral range, i.e. 4000-400/cm. To check the crystallinity and to measure average crystallite size of prepared nanoparticles XRD spectra was taken using JEOL (JSM-7600F, (XRD). For the study of surface morphology, mean diameter and shape of PdNPs, JSM-7600F, Japan (JEOL) field emission – scanning electron microscope FE-SEM was used.

2.4 Catalytic reduction of dyes

The photo catalytic performance of the PdNPs was evaluated by the degradation study of different dyes.

A known amount of PdNPs was added to the dye solution and irradiated with sunlight. The average temperature was 29°C. Before irradiation the mixture was stirred in the dark for 1h to get the absorption equilibrium between the dye and catalyst. A small amount of sodium borohydride reducing agent (1 mL, 10 mM) was added to the reaction mixture to initiate the photo-degradation process. The dye mixture was collected at definite time interval of irradiation and recorded the UV spectra to monitor the progress of the reaction. The stability of the PdNPs were investigated by the repeated cycles of photo-catalytic experiment.

3 Results and discussion

Guar gum was used as stabilizing agent for the synthesis of palladium nanoparticles. The formation of Nps were observed from color change and confirmed through UV spectrophotometer in the UV range of 300-700 nm. During the reaction the color of Pd (II), changes gradually from white to grey showing the Pd (0) formation. This color change is the result of SPR (surface Plasmon resonance, which is the excitations of surface electron on the conduction band) [43,44].

UV-vis spectra of guar gum in Figure 3 shows absorption peak at 299 nm while palladium chloride showed absorption at 470 nm. The change in absorption band of PdNPs in contrast to palladium chloride spectrum was ascribed to ligand-to-metal charge-transfer transitions of palladium (II) ion [45,46]

The peak of PdCl$_2$ at 470 nm gradually disappeared during the reaction that confirmed the formation of palladium nanoparticles, the color of solution also changes at this stage. For the reduction of Pd (II), no chemical reducing agent was used and the guar gum was used as stabilizing and reducing agent, which is green and non-toxic [29,47-49]. Guar gum is a high molecular weight polysaccharide and chemically consisting of
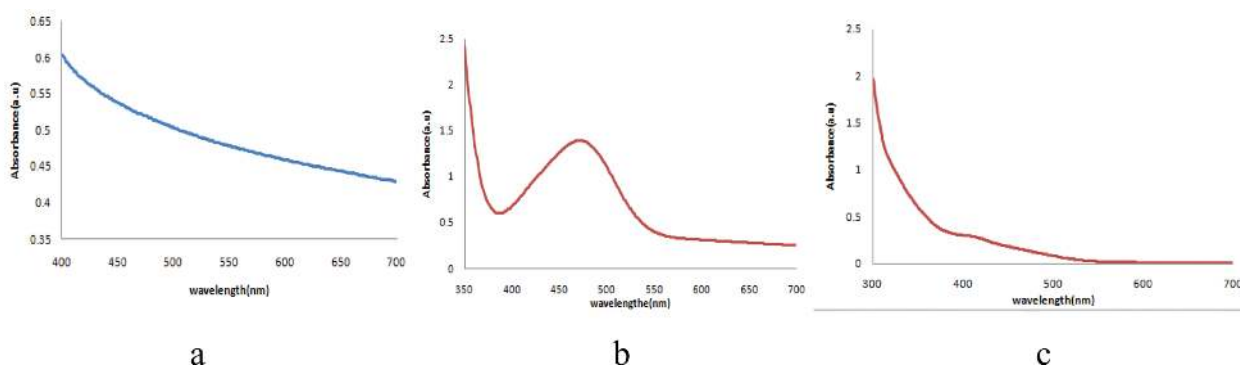
Figure 3: (a) UV-vis spectra of guar gum. (b) UV absorption peak of initial mixture before the reaction. (c) The formation of palladium nanoparticles, the peak at 470 nm gradually disappear after the reaction.
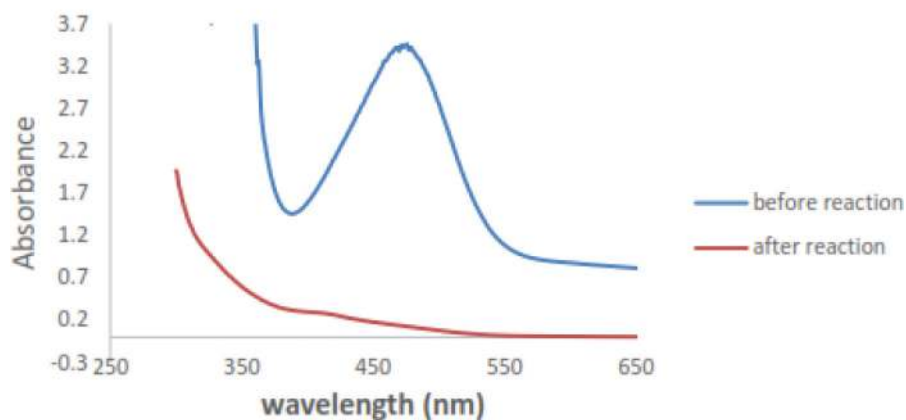

Figure 4: UV spectra before and after reaction, showing the formation of palladium nanoparticles.

sugar galactose and mannose molecules [50]. Hydroxyl group on the surface of guar gum are believed to be responsible for the Pd (II) reduction. The carboxylic and hydroxyl groups of guar gum form complex with Pd (II) ion and finally reduced it to Pd (0). Guar gum also contain starchy compound that act as stabilizing agent and help in prevention of PdNPs aggregation in water [12,51]. The change in UV spectra of reaction before and after the reaction can be observed in Figure 4.

3.1 FT-IR analysis

The formation of palladium nanoparticles were further confirm through FT-IR analysis. The FT-IR analysis (Figure 5 and Table 1) shows the presence of different functional groups in guar gum that are responsible for the stabilization and reduction of PdNPs. the major broad band at 3274 cm^{-1} corresponds to the −OH stretching. The weak peaks that appear at the 2745 cm^{-1} is assigned

to C−H stretching of the aliphatic groups of guar gum. The multiple bands at 2882 cm^{-1} showed the stretching vibrations of aromatic C−C bond. The strong and sharp peak at 1013 cm^{-1} corresponds to the C−O bond due to characteristic stretching of carbonyl and carboxylate groups.

The FT-IR analysis of PdNPs showed obvious changes in the peak position and intensity of the IR peaks of guar gum. These shifts in the peak position and intensity are due to the ligand-to-metal interaction and reduction of Pd (II) to Pd (0). In the PdNPs there is the formation of a new peak at 609 cm^{-1} along with the peaks of guar gum. This new peak corresponds to the M−O bond representing the interaction of Pd with the surface of guar gum and confirms the formation of nanoparticles. It confirms that there is a strong interaction among the different groups of guar gum and the metal. The absorption peak of hydroxal is shifted to 3265 cm^{-1}, the weak peak of −C−H stretching is now shifted to 2918 cm^{-1}, while the strong and sharp band at
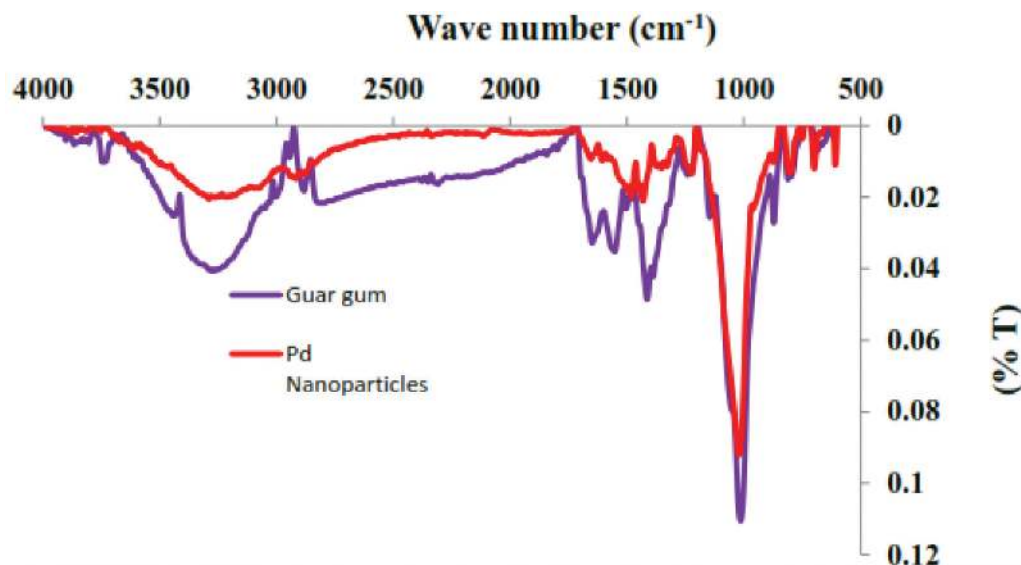
Figure 5: The combine FTIR spectra of guar gum and palladium nanoparticles.

Table 1: Different functional groups in gaur gum and their shift caused by palladium nanoparticles.

S.no	Peak position	Peak shift	Functional group	Remarks
1.	3440–3100 cm^{-1}	3500–3003 cm^{-1}	−OH	Broad and strong
2.	1649–1552 cm^{-1}	1481 cm^{-1}	−NH	W shape and weak
3.	1413 cm^{-1}	1431 cm^{-1}	−C−C− (aromatic ring)	Weak multiple peak
4.	1008 cm^{-1}	1020 cm^{-1}	−C=O	Strong and sharp peak

1013 cm^{-1} appeared at 1020 cm^{-1}. The peaks at 1222, 1350, 1431, 1485 and 1654 cm^{-1} due to the stretching of C−C bond while aromatic peaks at 811,700,609 cm^{-1} are also shifted in the presence of PdNPs. The above mentioned observation clearly indicated the interaction of Pd metal with −OH group of guar gum. It confirms that there is strong interaction among the different groups of guar gum like −OH, −COO^{-1}, −CO and palladium. This strong interaction results in the changes of the FT-IR spectra of guar gum both in position as well as intensity. All the above mentioned groups of guar gum have the ability to adsorb on the surface and stabilized the PdNPs. It is also worth mentioning that these groups bind to the metal nanoparticles and prevent its agglomeration in aqueous medium. Thus it is clear that guar gum has reduced and stabilized the palladium nanoparticles [52,53].

3.2 XRD analysis

The guar gum shows a broad reflection corresponding to the amorphous gum at 11.9825 and 14.62 position as shown in Figure 6. This pattern also shows large quantity of unreacted gum in our sample before the calcinations and sample is mostly in amorphous form [52].

XRD pattern after the calicination in Figure 7 shows the crystalline nature of synthesized PdNPS as all the peaks are clearly distinguishable. The peak at 33.85 is characteristics peak of the (111) indices of Pd (0). Two other peaks at 40.1 and 46.65 were observed that correspond to the reflection of (200) and (220) plane of crystal. Peak broadening was observed due to the effect of PdNPs. The crystallite size of prepared PdNPs was calculated by using the peak broadening profile of (111) peak at 39.81 by Sherrer's formula [54,55].

$$L = K\lambda/\beta_{1/2\,\cos\theta} \qquad (1)$$

where θ is the Bragg's angle, λ is the wave length (1.5418 Å) of the X-rays used, $\beta_{1/2}$ is the full peak width at half maximum (FWHM) of the diffraction profile in radians on a 2θ scale and K is constant equal to unit Y related to both crystal shape and the way θ is defined.

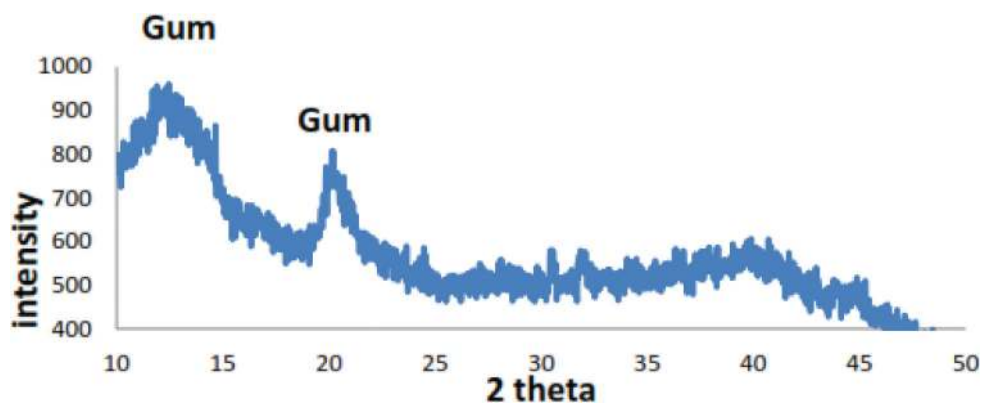The calculated crystallite size of the synthesized PdNPs is 10.

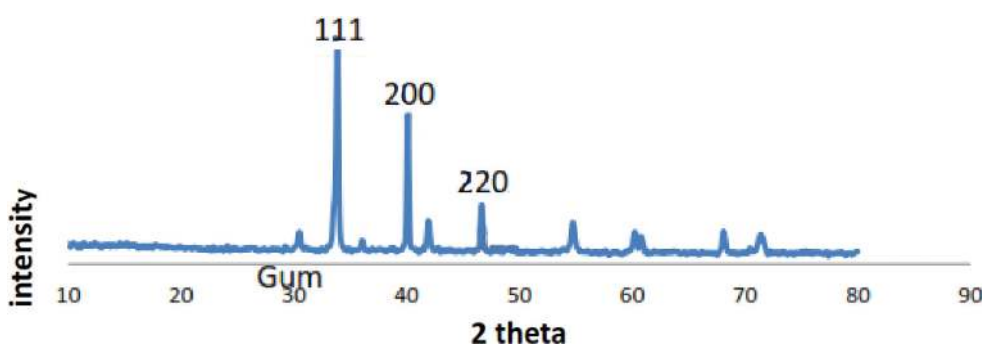**Figure 6:** The powder XRD (X-ray diffraction) pattern of the Pd-NPs/guar gum catalyst before the calcinations.

Figure 7: The powder XRD pattern of the Pd-NPs/guar gum catalyst after the calcinations.
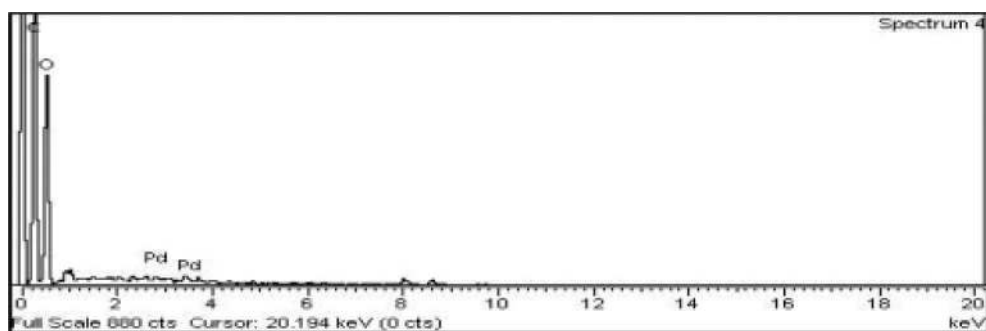

Figure 8: The EDX pattern of the synthesized palladium nanoparticles.

3.3 Elemental analysis

The peaks at 2.5 KeV and at 3.5 KeV (Figure 8) confirms the presence of palladium. Peaks at 0.3 KeV and 0.1 KeV confirm the presence of oxygen and carbon respectively. The presence of carbon is due to the organic compounds of guar gum while oxygen may be due to the compounds of guar gum as well as from the air. The elemental % composition is as Pd = 0.76%, C = 37.01% and O = 62.23%.

3.4 Morphological analysis

SEM analysis were performed for the study of surface of catalyst, morphology and size of prepared palladium nanoparticles, SEM images obtained for the green synthesized palladium nanoparticles (Figure 9) show that these particles are roughly spherical and also somewhat cubic within size range of 70-80 nm. The SEM image also revealed irregularly mono-dispersed palladium nanoparticles on the surface of guar gum matrix [56].

3.5 Catalytic activity of palladium nanoparticles

Palladium is one of the efficient but expensive hydrogenation catalysts. In order to determine the hydrogenation capacity and reusability of the prepared guar gum stabilized PdNPs, hydrogenation of para-nitrophenol using sodium borohydride as reducing agent was studied.

2 mL of para-nitrophenol was taken in quartz cuvettes; to this solution was added 1 mL of sodium borohydride (15 mM) solution. The para-nitrophenol showed strong absorption peak at 320 nm that was shifted to 401 nm when sodium borohydride was added. This shift in λ_{max} occurred due to the deprotonation of para-nitrophenol. On the addition of sodium borohydride the light color of para-nitrophenol changed to intense yellow that shows para-nitrophenolate ion formation. Sodium borohydride could not further reduce the phenolate ion even after 4 to 5 h. However when 10 µL palladium nano catalyst (0.2 mM) was

added to the above reaction mixture the peak intensity at 401 nm gradually decreased as the reaction time increases and a new absorption peak at 301 nm appeared that is due to the para-aminophenol formation. The reaction progress was monitored by UV-vis spectrophotometer and also observed visually when the yellow color of p-NP disappeared completely. This reaction was completed in 9 min at 27°C. The nitro compound like para-nitrophenol is usually reduced at high pressure or by using hydride donating compounds like $NaBH_4$ or $LiAlH_4$. These reagents alone are not as efficient to reduce para-nitrophenol at ordinary condition. Thus reducing power of this reagent can be enhanced by combining it with transition metal salt or halide, so we can say that NaBH4 is hydrogen source that releases hydrogen upon hydrolysis at ambient temperature. But need metals like palladium to reduced paranitrophenol completely to para-aminophenol [34,52,57,58]. Figure 10a shows the whole mechanism of reaction.

It is proposed that the decomposition of BH_4^- by PdNPs produces H-Pd and $PdBH_3^-$ as reactive intermediates:

$$2Pd + BH_4^- \leftrightarrow Pd - BH_3^- + Pd - H \tag{2}$$
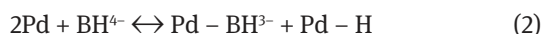
These active species are responsible for the conversion of 4-nitrophenol to 4-aminophenol stoichiometrically, for this conversion six-electron are needed.

$$6H - Pd + PNPs \rightarrow P\text{-}Ap + 6Pd + 6H \tag{3}$$
$$6Pd\text{-}BH_3 + P\text{-}NPs \rightarrow P\text{-}Ap + 6Pd + 6BH_3 \tag{4}$$
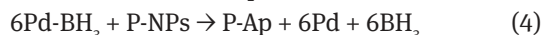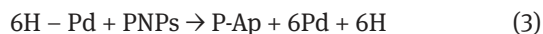
The results in Table 2 show promising improvement of the efficiency of catalyst as compared with the reported results in the literature.

Figure 11 shows the UV-vis spectra of 4-nitrophenol, reduction to 4- nitrophenolate ion with specific time interval and finally showed the formation of 4- aminophenol. The successive conversion percentage of para-nitrophenol to para-aminophenol was shown to be 90.93% (Figure 12).
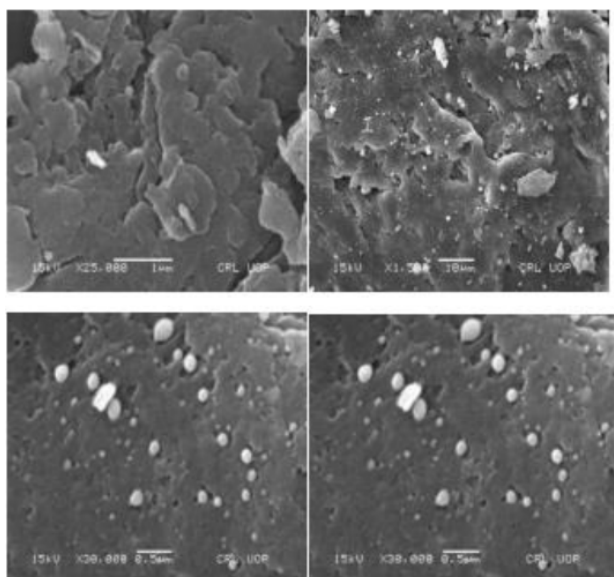

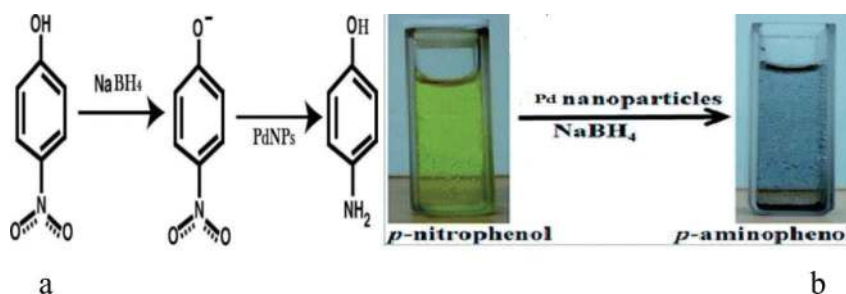**Figure 9:** The SEM image of palladium nanoparticles at different angles.

Figure 10: (a) Mechanism of the reaction. (b) Color changes in the reaction.

Figure 13 showed linear correlation between ln (A_o/A_t) verse time in minutes and the rate constant "K" for this reaction was found to be 0.049 min^{-1} for PdNPs stabilized by guar gum.

Table 2: Comparison of the results of this work with other reported methods in the reduction of 4-NP to 4-AP.

S.no	Catalyst used	Time of completion	Reference
1.	GA-Pt NPs	8 h	[59]
2.	Resin-Au NPs	20 min	[60]
3.	Ni-PVAm/SBA-15	85 min	[61]
4.	TiO$_2$-G1%	60 min	[62]
5.	Fe$_3$O$_4$@C@Pt	60 min	[63]
6.	Cu NPs	2 h	[64]
7.	HMMS-NH2-Pd	60 min	[65]
8.	Polymer-anchored Pd(II) complex	5.5 h	[66]
9.	PdCu/graphene	1.5 h	[67]
10.	Pd-NPs	9 min	Present work

The percent conversion of 4-nitrophenol was 90.93 that is calculated by following formula:

$$\alpha = (A_o - A_t)/A_o \times 100 \tag{5}$$

where α is the conversion percentage or efficiency of catalyst, A_o is initial absorption of 4-nitrophenol, and A_t is absorption of 4-nitrophenol at time t.

Turn over number (TON) is actually the mole of 4-nitrophenol obtained to the mole of palladium catalyst utilized in reduction. The Turn over number for the reaction is 27.78 that is calculated by following formula:

$$TON = \text{moles of 4-NP/moles of PdNPs} \times 100 \tag{6}$$

Turn over frequency is 185.2/h and is calculated by following formula:

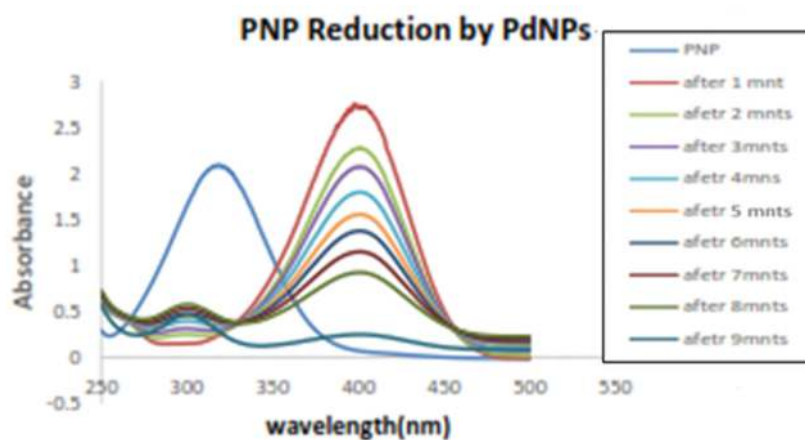$$TOF = TON/\text{Reaction time} \tag{7}$$

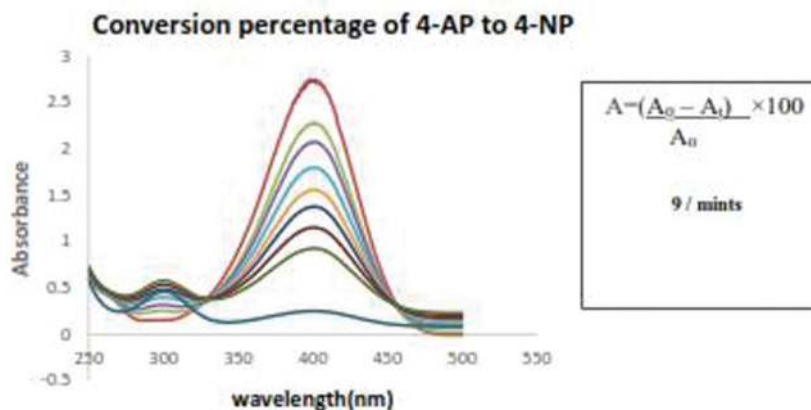**Figure 11:** 4NP reduction by PdNPs in 9 mints.

Figure 12: The successive conversion percentage of para-nitrophenol to para-aminophenol.
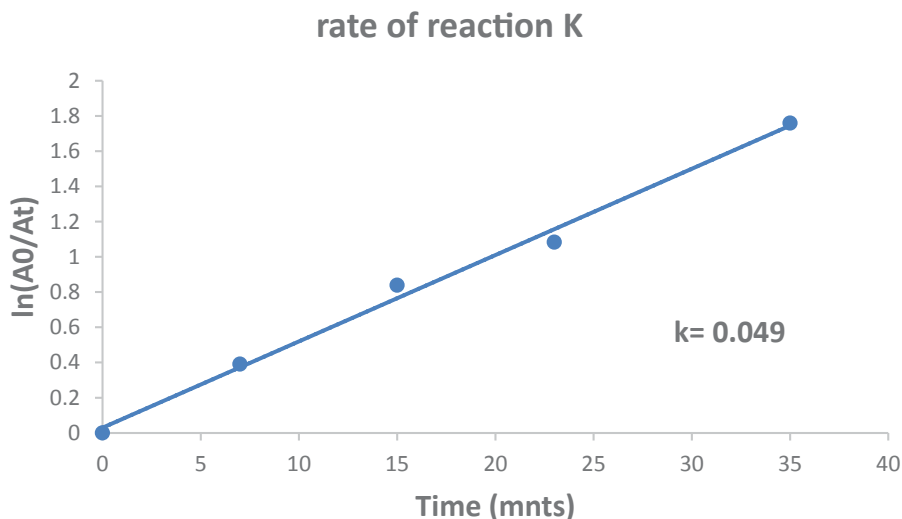
Figure 13: Rate constant K calculated for the reduction of para-nitrophenol.
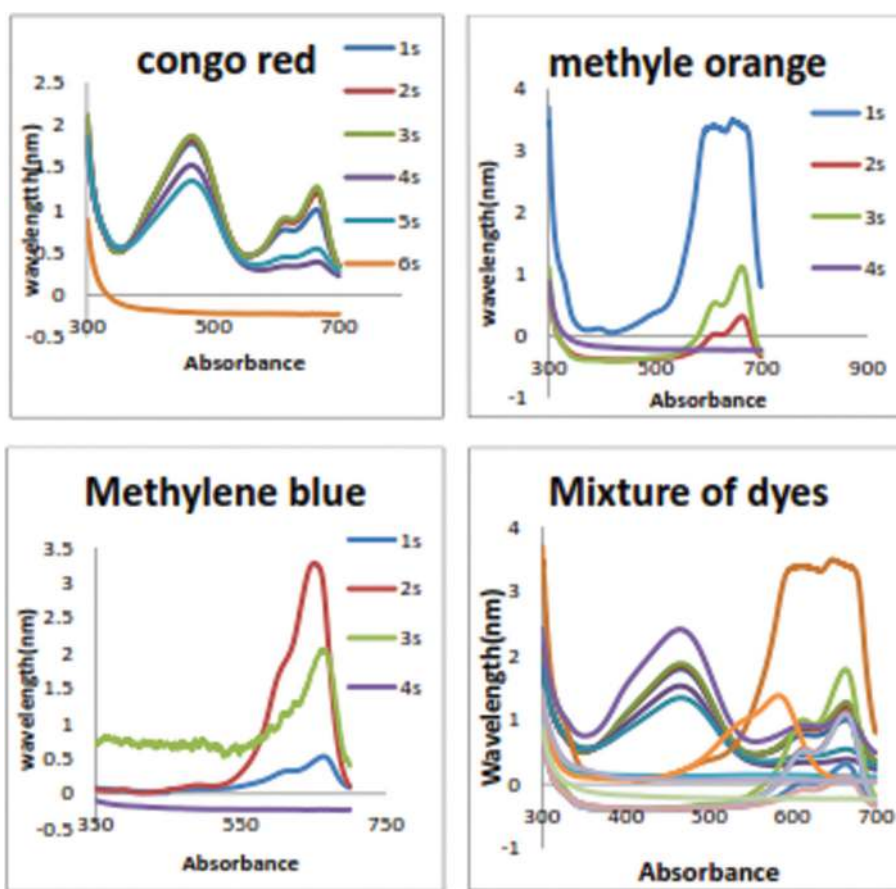
Figure 14: Catalytic activity of PdNPs in degradation of Congo red, methyl orange, methylene blue and mixture of the four different dyes.

3.5.1 Mercury drop test

In order to determine the nature of the catalyst mercury dropt test was performed. A solution of 4-nitrophenol was taken and added to it freshly prepared solution of $NaBH_4$, a red shift from 320 401 nm was observed due to the formation of phenolate ion. To this mixture added 0.001 g of the catalyst, the color of the mixture faded away gradually as the reaction proceeded which is due to the formation of 4-aminophenol showing a peak at 301 nm. When a drop of mercury was added with continuous stirring to this mixture, the color change stopped and the progress of the reaction

ceased, which was confirmed from the UV spectrum of the mixture after the addition of mercury. This indicated the formation of a Pd-mercury amalgam. This proves that the active catalytic specie under the reaction condition is the Pd (0), and the reaction occurs in a heterogeneous manner.

3.6 Catalytic reduction of methyl orange (MO), methyl blue (MB) and Congo red (CR)

The catalytic efficiency of the prepared PdNPS in the catalytic reduction was evaluated in the catalytic reduction of MO, MB, and CR and also in the mixture of all the three. The progress of reaction was monitored by UV spectrophotometer, as shown in the Figure 14. The above results illustrated that the prepared PdNPs are highly efficient in the reduction of CR, MB, MO and the mixture of all these three dyes by NaBH$_4$ aqueous solution. The comparison and efficiency of the prepared nanoparticles with the literature is given in Table 3. The reduction of MO, MB, CR and mixture were completed in 4 min, 4 min, 6 min and 6 min, respectively. The reduction rate of the catalyst prepared by using guar gum was comparable with our recently Published CuNPs catalyst.

3.7 Evaluation of the recyclability of the catalyst

According to industrial and commercial point of view, the recyclability is one of the most imperative factors

Table 3: Comparison of this work with reported work in the degradation of MB, MO, and CR.

Dye	Catalyst	Time	Reference
MB	Au/Fe$_3$O$_4$@C	600 s	[68]
	SiNWAS-Cu	600 s	[69]
	Porous Cu microspher	480 s	[70]
	PdNPs/guar gum	240 s	Present work
MO	Ag/TiO$_2$ nanocomposite	540 s	[71]
	CR Cu@SBA-15	300 s	[72]
	Ag/seashell	660 s	[73]
	Ag/Activated Carbon	420 s	[74]
	Ag/Tp	780 s	[75]
	AgCu/TP	300 s	[76]
	PdNPs/guar gum	240 s	Present work
CR	Cu Nanocrystal	500 s	[77]
	CR Cu@SBA-15	420 s	[72]
	Ag/Tp	1560 s	[74]
	AgCu/TP	420 s	[71]
	AgCu/GP	420 s	[73]
	PdNPs/guar gum	360 s	Present work

of heterogeneous catalyst. The reusability of prepared Pd-NPs was examined in reduction of P-NP to P-AP. After one complete reaction the catalyst was removed by mild centrifugation, washed with double distilled water, dried and used it again in reaction. The same catalyst was then repeatedly used for seven times in 100% reduction of P-nitrophenol and without any considerable loss of catalytic activity. Slight decline in efficiency was observed but after the 7th cycle as shown in Figure 15.
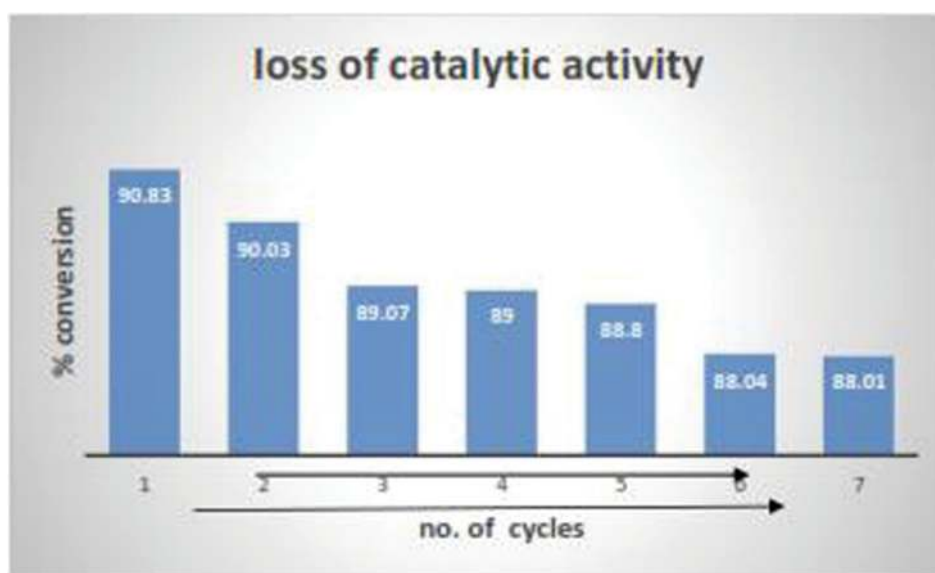

Figure 15: The loss of the catalytic activity of PdNPs on repeated cycle.

4 Conclusions

The palladium nanoparticles were prepared by using the guar gum as stabilizing and reducing agent. The prepared nanoparticles were then used for the reduction of P-NP, CR, MO, MB and mixture of these dyes. Results showed that PdNPs/guar gum have high catalytic efficiency in the reduction of above mentioned compounds. Furthermore, recycling of the catalyst also confirmed that prepared nanocatalyst is stable and could be recovered and reused for at least seven times for 100% reduction of organic dyes.

References

[1] Astruc D., Palladium Nanoparticles as Efficient Green Homogeneous and Heterogeneous Carbon–Carbon Coupling Precatalysts: A Unifying View. Inorg. Chem., 2007, 46(6), 1884-1894.

[2] Zhou W.P., Lewera A., Larsen R., Masel R.I., Bagus P.S., Wieckowski A., Size Effects in Electronic and Catalytic Properties of Unsupported Palladium Nanoparticles in Electrooxidation of Formic Acid. J. Phys. Chem., 2006, 110(27), 13393-13398.

[3] Antler M., The Development and Application of Palladium Contact Materials Recent Work on Telecommunications Connectors. Platin. Met. Rev., 1987, 31(1), 13-19.

[4] Steele B.C.H., Heinzel A., Materials for fuel-cell technologies. Nature, 2001, 414, 345.

[5] Weiss B.M., Iglesia E., Mechanism and site requirements for NO oxidation on Pd catalysts. J. Catal., 2010, 272(1), 74-81.

[6] Zhang X., Lee C.S.M., Mingos D.M.P., Hayward D.O., Oscillatory behaviour during the oxidation of methane over palladium metal catalysts. Appl. Catal. A, 2003, 240(1), 183-197.

[7] Brown W.H., Iverson B.L., Anslyn E., Foote C.S. Organic Chemistry (8th ed.). Brooks Cole, Belmont, USA, Mary Finch, 2017.

[8] Drahl C., Palladium's Hidden Talent. C&EN, 2008, 86(35), 53-56.

[9] Heck R.F., Nolley J.P., Palladium-catalyzed vinylic hydrogen substitution reactions with aryl, benzyl, and styryl halides. J. Org. Chem., 1972, 37(14), 2320-2322.

[10] Chen W., Shimada S., Tanaka M., Synthesis and Structure of Formally Hexavalent Palladium Complexes. Science, 2002, 295(5553), 308.

[11] Miyaura N., Yamada K., Suzuki A., A new stereospecific cross-coupling by the palladium-catalyzed reaction of 1-alkenylboranes with 1-alkenyl or 1-alkynyl halides. Tetrahedron Lett., 1979, 20(36), 3437-3440.

[12] Abad A., Almela C., Corma A., García H., Efficient chemoselective alcohol oxidation using oxygen as oxidant. Superior performance of gold over palladium catalysts. Tetrahedron Lett., 2006, 62(28), 6666-6672.

[13] Bianchini C., Shen P.K., Palladium-Based Electrocatalysts for Alcohol Oxidation in Half Cells and in Direct Alcohol Fuel Cells. Chem. Rev., 2009, 109(9), 4183-4206.

[14] Yousaf A.B., Imran M., Zaidi S.J., Kasak P., Ansari T.M., Manzoor S., et al., Synergistic effect of interfacial phenomenon on enhancing catalytic performance of Pd loaded $MnO_x–CeO_2–C$ hetero-nanostructure for hydrogenation and electrochemical reactions. J. Mater. Chem. A, 2017, 5(21), 10704-10712.

[15] Khodadadi B., Bordbar M., Yeganeh-Faal A., Optical, structural, and photocatalytic properties of Cd-doped ZnO powders prepared via sol–gel method. J. Sol-Gel. Sci. Techn., 2016, 77(3), 521-527.

[16] Khodadadi B., Sabeti M., Nahri-Niknafs B., Moradi-Dehaghi S., Aberomand-Azar P., Raeis-Farshid S., Preparation, characterization and photocatalytic activity of TiO_2/CoO nanocomposite. Bulg. Chem. Commun., 2014, 46(3), 624-628.

[17] Xin-ling G., Zheng-tao S., Research on preparation of nano-copper powder by liquid-phase method. Appl. Chem. Ind., 2005, 34(10), 615-617.

[18] Khodadadi B., Nickel doping effect on the photocatalytic activity of TiO_2/SiO_2 nanocomposite. Bulg. Chem. Commun., 2016, 48(2), 238-243.

[19] Khodadadi B., Effects of Ag, Nd codoping on structural, optical and photocatalytic properties of TiO_2 nanocomposite synthesized via sol-gel method using starch as a green additive. Iran. J. Catal., 2016, 6(3), 305-311.

[20] Laurent S., Forge D., Port M., Roch A., Robic C., Vander Elst L., et al., Magnetic iron oxide nanoparticles: synthesis, stabilization, vectorization, physicochemical characterizations, and biological applications. Chem. Rev., 2008, 108(6), 2064-2110.

[21] Suleiman M., Mousa M., Hussein A., Hammouti B., Hadda T.B., Warad I., Copper (II)-oxide nanostructures: synthesis, characterizations and their applications-review. J. Mater. Environ. Sci., 2013, 4(5), 792-797.

[22] Veisi H., Faraji A.R., Hemmati S., Gil A., Green synthesis of palladium nanoparticles using Pistacia atlantica kurdica gum and their catalytic performance in Mizoroki–Heck and Suzuki–Miyaura coupling reactions in aqueous solutions. Appl. Organomet. Chem., 2015, 29(8), 517-523.

[23] Okafor F., Janen A., Kukhtareva T., Edwards V., Curley M., Green synthesis of silver nanoparticles, their characterization, application and antibacterial activity. Int. J. Environ. Res. Pu., 2013, 10(10), 5221-5238.

[24] Sathishkumar M., Sneha K., Kwak I.S., Mao J., Tripathy S., Yun Y.-S., Phyto-crystallization of palladium through reduction process using Cinnamom zeylanicum bark extract. J. Hazard. Mater., 2009, 171(1-3), 400-404.

[25] Yang X., Li Q., Wang H., Huang J., Lin L., Wang W., et al., Green synthesis of palladium nanoparticles using broth of Cinnamomum camphora leaf. J. Nanopart. Res., 2010, 12(5), 1589-1598.

[26] Bankar A., Joshi B., Kumar A.R., Zinjarde S., Banana peel extract mediated novel route for the synthesis of palladium nanoparticles. Mater. Lett., 2010, 64(18), 1951-1953.

[27] Roopan S.M., Bharathi A., Kumar R., Khanna V.G., Prabhakarn A., Acaricidal, insecticidal, and larvicidal efficacy of aqueous extract of *Annona squamosa* L peel as biomaterial for the reduction of palladium salts into nanoparticles. Colloid. Surface B, 2012, 92, 209-212.

[28] Devi D.K., Pratap S.V., Haritha R., Sivudu K.S., Radhika P., Sreedhar B., Gum acacia as a facile reducing, stabilizing, and templating agent for palladium nanoparticles. J. Appl. Polym. Sci., 2011, 121(3), 1765-1773.

[29] Sheny D., Philip D., Mathew J., Rapid green synthesis of palladium nanoparticles using the dried leaf of *Anacardium occidentale*. Spectrochimica Acta A Mol. Biomol. Spectrosc., 2012, 91, 35-38.

[30] Khan M., Khan M., Kuniyil M., Adil S.F., Al-Warthan A., Alkhathlan H.Z., et al., Biogenic synthesis of palladium nanoparticles using *Pulicaria glutinosa* extract and their catalytic activity towards the Suzuki coupling reaction. Dalton T., 2014, 43(24), 9026-9031.

[31] Baran T., Biosynthesis of Highly Retrievable Magnetic Palladium Nanoparticles Stabilized on Bio-composite for Production of Various Biaryl Compounds and Catalytic Reduction of 4-Nitrophenol. Catal. Lett., 2019, 149(6), 1721-1729.

[32] Baran T., Menteş A., Construction of new biopolymer (chitosan)-based pincer-type Pd (II) complex and its catalytic application in Suzuki cross coupling reactions. J. Mol. Struct., 2017, 1134, 591-598.

[33] Venkatesham M., Ayodhya D., Veerabhadram G., Green synthesis, characterization and catalytic activity of palladium nanoparticles by xanthan gum. Appl. Nanosci., 2015, 5(3), 315-320.

[34] Zhang P., Shao C., Zhang Z., Zhang M., Mu J., Guo Z., et al., In situ assembly of well-dispersed Ag nanoparticles (AgNPs) on electrospun carbon nanofibers (CNFs) for catalytic reduction of 4-nitrophenol. Nanoscale, 2011, 3(8), 3357-3363.

[35] Saha S., Pal A., Kundu S., Basu S., Pal T., Photochemical green synthesis of calcium-alginate-stabilized Ag and Au nanoparticles and their catalytic application to 4-nitrophenol reduction. Langmuir, 2009, 26(4), 2885-2893.

[36] Kuroda K., Ishida T., Haruta M., Reduction of 4-nitrophenol to 4-aminophenol over Au nanoparticles deposited on PMMA. J. Mol. Catal. A-Chem., 2009, 298(1-2), 7-11.

[37] Qiu L., Peng Y., Liu B., Lin B., Peng Y., Malik M.J., et al., Polypyrrole nanotube-supported gold nanoparticles: An efficient electrocatalyst for oxygen reduction and catalytic reduction of 4-nitrophenol. Appl. Catal. A, 2012, 413, 230-237.

[38] Dubey S.P., Dwivedi A.D., Kim I.-C., Sillanpaa M., Kwon Y.-N., Lee C., Synthesis of graphene–carbon sphere hybrid aerogel with silver nanoparticles and its catalytic and adsorption applications. Chem. Eng. J., 2014, 244, 160-167.

[39] Lin D.-H., Jiang Y.-X., Wang Y., Sun S.-G., Silver nanoparticles confined in SBA-15 mesoporous silica and the application as a sensor for detecting hydrogen peroxide. J. Nanomater., 2008, 2008, 12.

[40] Hwang C.-G., Sang-Ho K., Hoon O.J., Kim M.-R., Choi S.-H., Reduction of aromatic nitro compounds on Pd colloids prepared by γ-irradiation. J. Ind. Eng. Chem., 2008, 14(6), 864-868.

[41] Jan J.-S., Chuang T.-H., Chen P.-J., Teng H., Layer-by-layer polypeptide macromolecular assemblies-mediated synthesis of mesoporous silica and gold nanoparticle/mesoporous silica tubular nanostructures. Langmuir, 2011, 27(6), 2834-2843.

[42] Veisia H., Farajib A.R., Hemmatia S., Gil A., Green synthesis of palladium nanoparticles using Pistacia atlantica kurdica gum and their catalytic performance in Mizoroki–Heck and Suzuki–Miyaura coupling reactions in aqueous solutions. Appl. Organometal. Chem., 2015, 29(8), 517-523.

[43] He F., Liu J., Roberts C.B., Zhao D., One-Step "Green" Synthesis of Pd Nanoparticles of Controlled Size and Their Catalytic Activity for Trichloroethene Hydrodechlorination. Ind. Eng. Chem. Res., 2009, 48(14), 6550-6557.

[44] Gonzalez A., Noguez C., Influence of Morphology on the Optical Properties of Metal Nanoparticles. J. Comput. Theor. Nanos., 2007, 4, 231-238.

[45] Kim J.Y., Kim M., Kim H.M., Joo J., Choi J.H., Electrical and optical studies of organic light emitting devices using SWCNTs-polymer nanocomposites. Opt. Mater., 2003, 21(1-3), 147-151.

[46] Schultz D.A., Plasmon resonant particles for biological detection. Curr. Opin. Biotech., 2003, 14(1), 13-22.

[47] Nadagouda M.N., Varma R.S., Green synthesis of silver and palladium nanoparticles at room temperature using coffee and tea extract. Green Chem., 2008, 10(8), 859-862.

[48] Nemamcha A., Rehspringer J.-L., Khatmi D., Synthesis of Palladium Nanoparticles by Sonochemical Reduction of Palladium(II) Nitrate in Aqueous Solution. J. Phys. Chem. B, 2006, 110(1), 383-387.

[49] Namini P.A., Babaluo A.A., Bayati B., Palladium nanoparticles synthesis using polymeric matrix: poly(ethyleneglycol) molecular weight and palladium concentration effects. Int. J. Nanosci. Nanotechno., 2007, 3(1), 37-44.

[50] Mudgil D., Barak S., Khatkar B.S., Guar gum: processing, properties and food applications-A Review. J. Food Sci. Technol., 2014, 51(3), 409-418.

[51] Stahl S., Palladium Reagents and Catalysts. New Perspectives for the 21st Century, 2005, 997-998.

[52] Santoshi kumari A., Venkatesham M., Ayodhya D., Veerabhadram G., Green synthesis, characterization and catalytic activity of palladium nanoparticles by xanthan gum. Appl. Nanosci., 2015, 5(3), 315-320.

[53] Venkatesham M., Ayodhya D., Madhusudhan A., Veera Babu N., Veerabhadram G., A novel green one-step synthesis of silver nanoparticles using chitosan: catalytic activity and antimicrobial studies. Appl. Nanosci., 2014, 4(1), 113-119.

[54] Lishan J., Qian Z., Qingbiao L., Hao S., The biosynthesis of palladium nanoparticles by antioxidants in *Gardenia jasminoides* Ellis: long lifetime nanocatalysts for p-nitrotoluene hydrogenation. Nanotechnology, 2009, 20(38), 385601.

[55] Jain P.K., Huang X., El-Sayed I.H., El-Sayed M.A., Noble Metals on the Nanoscale: Optical and Photothermal Properties and Some Applications in Imaging, Sensing, Biology, and Medicine. Accounts Chem. Res., 2008, 41(12), 1578-1586.

[56] Khazaei A., Rahmati S., Ghaderi A., Roshan L., Palladium nanoparticles supported on gum arabic as a reusablecatalyst for solvent-free Mizoroki-Heck reaction. J. Iran. Chem. Soc., 2014, 11, 263-269.

[57] Saha S., Pal A., Kundu S., Basu S., Pal T., Photochemical Green Synthesis of Calcium-Alginate-Stabilized Ag and Au Nanoparticles and Their Catalytic Application to 4-Nitrophenol Reduction. Langmuir, 2010, 26(4), 2885-2893.

[58] Kuroda K., Ishida T., Haruta M., Reduction of 4-nitrophenol to 4-aminophenol over Au nanoparticles deposited on PMMA. J. Mol. Catal. A-Chem., 2009, 298(1), 7-11.

[59] Sreedhar B., Devi D.K., Yada D., Selective hydrogenation of nitroarenes using gum acacia supported Pt colloid an effective reusable catalyst in aqueous medium. Catal. Commun., 2011, 12(11), 1009-1014.

[60] Shah D., Kaur H., Resin-trapped gold nanoparticles: An efficient catalyst for reduction of nitro compounds and Suzuki-Miyaura coupling. J. Mol. Catal A-Chem., 2014, 381, 70-76.

[61] Kalbasi R.J., Nourbakhsh A.A., Babaknezhad F., Synthesis and characterization of Ni nanoparticles-polyvinylamine/SBA-15 catalyst for simple reduction of aromatic nitro compounds. Catal. Commun., 2011, 12(11), 955-960.

[62] Xu C., Yuan Y., Yuan R., Fu X., Enhanced photocatalytic performances of TiO_2-graphene hybrids on nitro-aromatics reduction to amino-aromatics. RSC Adv., 2013, 3(39), 18002-18008.

[63] Xie M., Zhang F., Long Y., Ma J., Pt nanoparticles supported on carbon coated magnetic microparticles: an efficient recyclable catalyst for hydrogenation of aromatic nitro-compounds. RSC Adv., 2013, 3(26), 10329-10334.

[64] Duan Z., Ma G., Zhang W., Preparation of copper nanoparticles and catalytic properties for the reduction of aromatic nitro compounds. Bull. Korean., Chem. Soc., 2012, 33(12), 4003-4006.

[65] Wang P., Zhang F., Long Y., Xie M., Li R., Ma J., Stabilizing Pd on the surface of hollow magnetic mesoporous spheres: A highly active and recyclable catalyst for hydrogenation and Suzuki coupling reactions. Catal. Sci. Technol., 2013, 3(6), 1618-1624.

[66] Islam M., Mondal P., Roy A.S., Tuhina K., Synthesis, characterization and catalytic activities of a reusable polymer-anchored palladium (II) complex: effective catalytic hydrogenation of various organic substrates. Transit. Metal Chem., 2010, 35(4), 427-435.

[67] Shil A.K., Sharma D., Guha N.R., Das P., Solid supported Pd (0): an efficient recyclable heterogeneous catalyst for chemoselective reduction of nitroarenes. Tetrahedron Lett., 2012, 53(36), 4858-4861.

[68] Gan Z., Zhao A., Zhang M., Tao W., Guo H., Gao Q., et al., Controlled synthesis of Au-loaded Fe_3O_4@C composite microspheres with superior SERS detection and catalytic degradation abilities for organic dyes. Dalton T., 2013, 42(24), 8597-8605.

[69] Yang X., Zhong H., Zhu Y., Jiang H., Shen J., Huang J., et al., Highly efficient reusable catalyst based on silicon nanowire arrays decorated with copper nanoparticles. J. Mater. Chem. A, 2014, 2(24), 9040-9047.

[70] Zhang Y., Zhu P., Chen L., Li G., Zhou F., Lu D.D., et al., Hierarchical architectures of monodisperse porous Cu microspheres: synthesis, growth mechanism, high-efficiency and recyclable catalytic performance. J. Mater. Chem. A, 2014, 2(30), 11966-11973.

[71] Atarod M., Nasrollahzadeh M., Sajadi S.M., *Euphorbia heterophylla* leaf extract mediated green synthesis of Ag/TiO_2 nanocomposite and investigation of its excellent catalytic activity for reduction of variety of dyes in water. J. Colloid. Interf. Sci., 2016, 462, 272-279.

[72] Ghosh B.K., Hazra S., Naik B., Ghosh N.N., Preparation of Cu nanoparticle loaded SBA-15 and their excellent catalytic activity in reduction of variety of dyes. Powder Technol., 2015, 269, 371-378.

[73] Rostami-Vartooni A., Nasrollahzadeh M., Alizadeh M., Green synthesis of seashell supported silver nanoparticles using *Bunium persicum* seeds extract: application of the particles for catalytic reduction of organic dyes. J. Colloid. Interf. Sci., 2016, 470, 268-275.

[74] Nasrollahzadeh M., Sajadi S.M., Hatamifard A., Waste chicken eggshell as a natural valuable resource and environmentally benign support for biosynthesis of catalytically active Cu/eggshell, Fe_3O_4/eggshell and Cu/Fe_3O_4/eggshell nanocomposites. Appl. Catal. B- Environ., 2016, 191, 209-227.

[75] Khan S.A., Ismail M., Anwar Y., Farooq A., Al Johny B.O., Akhtar K., et al., A highly efficient and multifunctional biomass supporting Ag, Ni, and Cu nanoparticles through wetness impregnation for environmental remediation. Green Process. Synth., 2019, 8(1), 309-319.

[76] Ismail M., Khan M., Khan S.A., Qayum M., Khan M.A., Anwar Y., et al., Green synthesis of antibacterial bimetallic Ag–Cu nanoparticles for catalytic reduction of persistent organic pollutants. J. Mater. Sci.-Mater. El., 2018, 29(24), 20840-20855.

[77] Zhang P., Sui Y., Wang C., Wang Y., Cui G., Wang C., et al., A one-step green route to synthesize copper nanocrystals and their applications in catalysis and surface enhanced Raman scattering. Nanoscale, 2014, 6(10), 5343-5350.